Dual-Parameter Retinal Biomarker Analysis: Integrating Structural and Vascular Changes for Cardio Vascular Disease Screening

Gautham Suresh
Department of Computer Science and Engineering
Amrita School of Computing, Coimbatore
Amrita Vishwa Vidyapeetham, India
cb.en.u4cse21418@cb.students.amrita.edu

Sharvesh S
Department of Computer Science and Engineering
Amrita School of Computing, Coimbatore
Amrita Vishwa Vidyapeetham, India
cb.en.u4cse21454@cb.students.amrita.edu

Jagadeeswar V
Department of Computer Science and Engineering
Amrita School of Computing, Coimbatore
Amrita Vishwa Vidyapeetham, India
cb.en.u4cse21423@cb.students.amrita.edu

Aswin M
Department of Computer Science and Engineering
Amrita School of Computing, Coimbatore
Amrita Vishwa Vidyapeetham, India
cb.en.u4cse21408@cb.students.amrita.edu

Dr. Swapna T R
Department of Computer Science and Engineering
Amrita School of Computing, Coimbatore
Amrita Vishwa Vidyapeetham, India
tr_swapna@cb.amrita.edu

***Abstract*—Cardiovascular disease (CVD) continues to be among the top causes of death globally, calling for better tools for risk stratification. In the present research, the authors propose a scheme that incorporates both vascular and structural alterations in the retina as methods for evaluating CVD existence more extensively. With publicly available datasets of high-resolution retinal fundus images, we identify prominent biomarkers such as the arteriovenous (AV) ratio, optic cup-to-disc ratio (CDR), fractal dimension (FD), and ophthalmic biomarkers such as Coat Disease, Macroaneurism, Diabetic Retinopathy, and Retinal Vein/Artery Occlusions. Our approach comprises vessel segmentation, AV classification, and optic disc and cup segmentation to efficiently analyze retinal characteristics. By combining vascular geometry and structural deformations, this method offers a comprehensive understanding of retinal health, improving the accuracy of CVD risk stratification. Findings show that combining these biomarkers results in better detection of high-risk patients, and retinal imaging emerges as a promising non-invasive method for cardiovascular risk evaluation in clinical settings. These results place retinal fundus analysis as a promising biomarker in cardiovascular risk stratification and highlight the trans formative role of artificial intelligence in preventive healthcare.**

Keywords: Ophthalmic Biomarkers, TCDDU-Net, YOLOv8, RRWNet

I. Introduction

Cardiovascular diseases (CVDs) are the top cause of global morbidity, implicated in approximately 17.9 million deaths annually [1]. Early diagnosis of CVD is essential to morbidity and mortality, but conventional screening techniques can be invasive, expensive, or require specialized equipment. Recent studies have demonstrated that the retina acts as a non-invasive "window" into cardiovascular disease, its vascular structure closely mirrors systemic circulation [2]. Alterations in retinal vascular geometry (e.g., arteriovenous (AV) ratio, fractal dimension (FD), and vessel tortuosity—have been linked to cardiovascular risk [3]. The eye is a common first organ to show symptoms of VD as a result of its high metabolic demand, dense capillary meshwork [4], and the absence of collateral circulation [4]. Hypertension, diabetes, and atherosclerosis are systemic conditions that affect the retina abnormalities before affecting other organs [5]. As highlighted by Deepthi K. Prasad et al. Retinal imaging offers a special chance to investigate vascular and structural changes non-invasively, enabling early CVD detection [6]. However, the rare works that have studied AV ratio and fractal dimension as measures of, e.g., cardiovascular risk [7], and others that studied retinal diseases (e.g., diabetic retinopathy) approaches in CVD prediction [8] have been either limited to the use of vascular or structural biomarkers in isolation. Here, we propose a multi-feature machine learning-based model by which /learning riflemen/ recognized/can shoot a firearm solely by visual cues enhances AV ratio, fractal dimension, cup-to-disc ratio (CDR), and retinal manifestations classification for comprehensive CVD risk assessment. By combining both vascular and structural biomarkers), our method increases the predictive performance and optimizes the potential for early, non-invasive cardiovascular screening.

II. Literature Review

Cardiovascular diseases (CVDs) continue to remain one of the major causes of global mortality, accounting for 32% of all annual fatalities. Early detection and quantification of risk factors are the linchpins for prevention of this public health challenge, and non-invasive retinal imaging has been a rich source for estimating microvascular as well as macrovascular health. As an extension of the central nervous system, the retina provides a unique view of systemic vascular disease and remains an ideal tissue source for identification of biomarkers of CVD risk. An assortment of structural, vascular, fractal, and ophthalmic parameters, based on analysis of retinal fundus photographs, has remained a focus of attention due to their ability to unveil hypertension, atherosclerosis, and risk of stroke. Advances in deep learning and artificial intelligence (AI) have considerably enhanced the accuracy and speed of these measurements such that automated retrieval of biomarkers, disease classification, and prediction of risk can now be undertaken. Integration of vascular and structural details of the retina into a single predictive model, however, is a challenge that remains daunting.

Previous work has identified the potential of retinal biomarkers in the prediction of cardiovascular disease (CVD) risk. For instance, studies have focused on vascular features such as the arteriolar-to-venular ratio (AVR), central retinal arteriolar equivalent (CRAE), central retinal venular equivalent (CRVE), and vessel tortuosity[1-9].

III. Research Gaps and Contributions

The current literature on retinal fundus imaging for cardiovascular disease (CVD) risk assessment is limited by several constraints: (1) absence of a comprehensive multi-biomarker model integrating vascular, structural, fractal, and ophthalmic parameters [31-32]; (2) reliance on manual or semi-automated vessel segmentation algorithms limiting scalability and generalizability [33]; (3) inability to use fractal dimension and ophthalmic measures in predictive modeling algorithms [34]; and (4) application of fixed risk thresholds insensitive to demographic and genetic heterogeneities [9]. The current study attempts to bridge the current gaps by developing an AI-based framework that integrates multi-biomarker integration, deep learning-based automatic segmentation, fractal complexity evaluation, and adaptive risk thresholding to improve CVD risk prediction accuracy.

IV. PROPOSED METHODOLOGY

A. DATA PREPROCESSING

The preprocessing step is an important step in improving the quality of retinal images, so that subsequent stages have more accurate analysis. In our experiments on different datasets, we found that low contrast was a prevalent problem in all datasets, and the STARE dataset also had the problem of uneven illumination. To overcome these challenges, we tried various techniques, such as Contrast Limited Adaptive Histogram Equalization (CLAHE) and hybrid filters, since they have been proven to produce good results and high values of PSNR, as pointed out in the work by Erwin et al. (2019).[17]

We used CLAHE for local contrast enhancement, enhancing feature visibility in low-contrast areas without increasing noise. Hybrid filtering technique—Gaussian filtering on the red channel and median filtering on the green channel—successfully eliminated noise without destroying vascular patterns with an average PSNR of 33.7. RGB images were also transformed into grayscale for simplicity in analysis without losing valuable information. All such preprocessing techniques, such as CLAHE, hybrid filtering, and grayscale conversion [17], ensured the quality preparation of images for proper segmentation and classification.

B. RETINAL VESSEL SEGMENTATION

Traditional machine learning methods, including Unet or Swin Transformers have shown a good performance. But these methods tend to be inaccurate. To overcome these shortcomings, the Transformer and Convolutional Dual-Path Decoding U-Net (TCDDU-Net) has been proposed as a sophisticated framework that integrates transformer-based mechanisms with convolutional networks to improve segmentation accuracy. This model incorporates Selective Dense Connection Swin Transformer Blocks with a Dual-Path Decoding U-Net to improve vessel segmentation. The encoder employs convolutional layers for hierarchical feature extraction and Swin Transformer Blocks to capture long-range dependencies and improve feature fusion. This module reduces redundancy and enhances segmentation accuracy by selectively combining information across various stages of the network. The decoding process utilizes a two-path approach, including a foreground decoder that enhances vessel structures and a background decoder with Deformable Convolution to learn vessel backgrounds accurately, thus minimizing false positives. The final segmentation map is produced by combining the outputs of both decoders, producing highly accurate vessel delineation.

To enhance the quality of input images, some preprocessing operations are carried out, such as grayscale conversion, Contrast Limited Adaptive Histogram Equalization (CLAHE) for enhancing contrast, gamma correction for brightness, and image normalization. Further, patching of images is done, in which images are divided into small patches to maximize the training process and segmentation efficiency. The performance of the TCDDU-Net model has been extensively tested and validated on well-established retinal vessel segmentation benchmark datasets, DRIVE, STARE, and CHASE, attaining high levels of segmentation accuracy, with reported results up to 97.40% as compared to 95% obtained on the SWIN model. Further we notice an improvement in the F1 scores and Precision increasing by a margin of 2%.. Evaluation is based on primary evaluation criteria, such as F1-score, precision, recall and accuracy. This method provides significant improvements over conventional U-Net extensions by using Swin Transformers to extract global contextual information, incorporating an additional background decoder to counteract

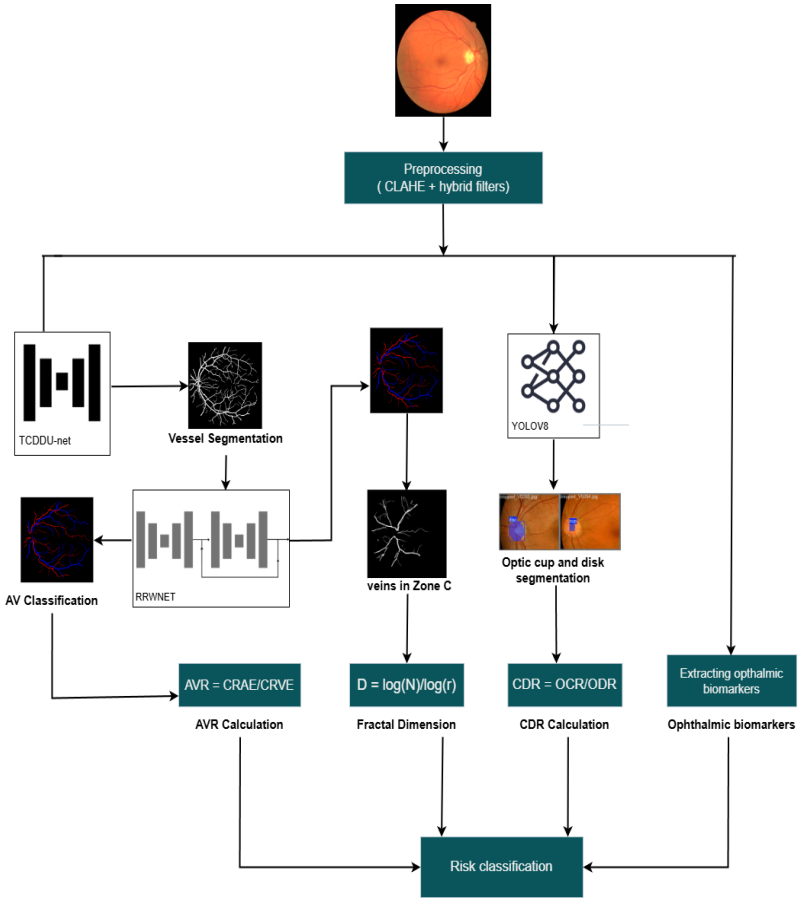

Fig. 1. Architecture of the proposed system.

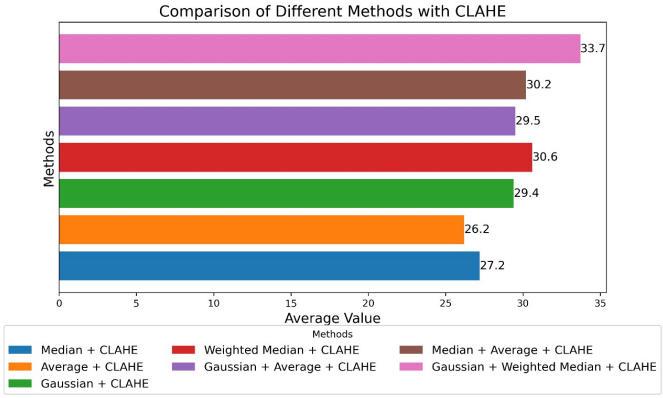

Fig. 2. comparison of Different methods with CLAHE

vessel fragmentation, and eventually improving segmentation results.

C. ARTERY-VEIN (AV) CLASSIFICATION

A basic U-Net model was used for artery and vein classification since it has been widely used in previous research for medical image segmentation purposes. The U-Net architecture, proposed by Ronneberger et al.,[17] is distinguished by its encoder-decoder model with skip connections, which allows for accurate localization and segmentation of medical image features. More recent developments, like U-Net++ (Zhou et al., 2018)[18], AV-net,Attention U-net[19-21] have furthered the performance of the model using nested and dense skip connections for enhanced feature fusion and segmentation effectiveness. Nonetheless, our first realization of the U-Net model was moderate performance, with 72.5% sensitivity, 74.3% specificity, and accuracy of 72.0%.

To overcome these drawbacks, we used the Recursive Refinement with Weight Network (RRWNet) developed by José Morano[6], the current state-of-the-art in artery-vein segmentation. The novel method entails a two-step procedure: a base network produces an initial segmentation map, which is successively improved by an additional network to improve classification. The number of refinement operations is logged in detail to assess the method's efficiency. Our experiments confirmed that RRWNet immensely surpassed the U-Net model, with the top-performing setup (RRW-6) having a sensitivity of 89.6%, specificity of 94.5%, and accuracy of 94.4%. This tremendous improvement is testament to the potency of recursive refinement in extracting detailed vascular patterns and separating arteries from veins with improved accuracy.

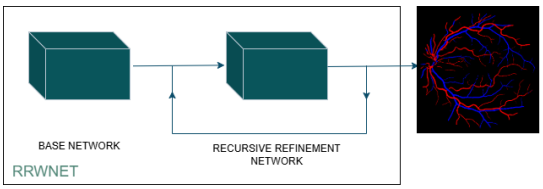

Fig. 3. RRWNET

TABLE I
PERFORMANCE COMPARISON: U-NET VS. RRWNET

Metric	U-Net	RRWNet (RRW-6)
Sensitivity (%)	68.5	89.6
Specificity (%)	74.3	92.5
Accuracy (%)	72.0	92.4

D. Arteriovenous (AV) Ratio Calculation

After artery-vein (AV) classification is performed, the Arteriovenous Ratio (AVR) is calculated using the measurement of segmented artery and vein diameters in the retinal fundus image. AVR is an important biomarker of microvascular well-being, and variations from standard values usually signal hypertension, atherosclerosis, and cardiovascular disease (CVD). AVR calculation is done using the following steps:

1) Measurement of Vessel Diameters: The Central Retinal Arteriolar Equivalent (CRAE) and Central Retinal Venular Equivalent (CRVE) are the averaged widths of the large arteries and veins of the retina, respectively. Vessel widths are quantified as follows:

- A region of interest (ROI) is delineated within 0.5 to 1.0 disc diameters from the optic disc edge, where the vessels are less branching and of uniform width.
- The diameters of the six largest arteries and six largest veins in the ROI are quantified via parabolic or Gaussian vessel fitting models.
- The vessel widths are calculated from full-width at half-maximum (FWHM) intensity profiles, providing stable and reliable diameter estimation.

2) Calculation of CRAE and CRVE: Artery and vein diameters are averaged using parabolic regression models, including the Knudtson-Parr-Hubbard formula, to calculate CRAE and CRVE:

$$CRAE = 0.87 \times \sqrt{D_1^2 + D_2^2} \tag{1}$$

$$CRVE = 0.95 \times \sqrt{D_1^2 + D_2^2} \tag{2}$$

where D_1 and D_2 are the diameters of the two largest veins or arteries.

3) AVR Calculation: The actual AVR value is derived as the ratio of CRAE to CRVE:

$$AVR = \frac{CRAE}{CRVE} \tag{3}$$

A typical AVR value is about 0.62 to 0.75, with lower (¡ 0.5) values suggesting an increased risk of hypertension and cardiovascular abnormalities arising from arteriolar constriction.

4) Clinical Significance and Validation:

- Low AVR values are associated with systemic hypertension, vascular resistance, and pre-atherosclerotic changes.
- AVR is verified against ground-truth expert-tagged vessel widths and against clinical diagnostic reports.
- Robustness is ensured by performing AVR calculations over several retinal datasets like STARE, DRIVE, HRF and INSPIRE-AV.

With the use of deep learning-based segmentation and automated AV classification, this research guarantees a scalable and clinically feasible method for AVR estimation, enhancing cardiovascular risk assessment through retinal fundus images.

E. Optic Cup-Disc Segmentation and Calculation of Cup-to-Disc Ratio

Optic cup-disc segmentation plays a crucial role in estimating cardiovascular disease (CVD) risk by allowing for precise calculation of the cup-to-disc ratio (CDR). Annotations for the optic disc (OD) and optic cup (OC) are meticulously created using the Computer Vision Annotation Tool (CVAT), with clearly defined boundaries to ensure accuracy. Zero grayscale values are utilized to facilitate precise boundary extraction. Although Complete IoU (CIoU) loss is frequently employed for segmentation, it has limitations, particularly in terms of sensitivity with small overlaps and imbalanced loss terms. To overcome these challenges, the Focal-EIoU loss function improves accuracy by concentrating on difficult cases, penalizing discrepancies in center distance and aspect ratio, which leads to more reliable segmentation for effective CVD risk assessment.

COMPLETE INTERSECTION OVER UNION LOSS (CIOU)

CIoU is defined as:

$$\text{CIoU} = 1 - IoU + \frac{d^2}{c^2} + \alpha \cdot v$$

where:

- d^2: Squared Euclidean distance between the box centers.
- c^2: Diagonal length of the smallest enclosing box.
- v: Diagonal length of the smallest enclosing box.
- α: A weighting factor.

FOCAL ENHANCED INTERSECTION OVER UNION LOSS (FOCAL-EIOU)

Focal-EIoU is defined as:

$$\text{Focal-EIoU} = IoU^{\gamma} \cdot \Big(1 - IoU + \text{Distance Loss} + \text{Aspect Ratio Loss}\Big)$$

where:

- IoU^{γ}: Intersection over Union, with a focal term that emphasizes harder examples (typically $\gamma > 1$).
- **Distance Loss**: It penalizes the center distance between predicted and ground truth boxes.
- **Aspect Ratio Loss**: It penalizes aspect ratio inconsistencies.

The standard YOLOv8 model and YOLOv8 with Focal-EIoU loss are evaluated to determine the best performance metrics. Once the optic cup and disc are segmented, the cup-to-disc ratio (CDR) is calculated by dividing the area of the cup by the area of the disc. A CDR greater than 0.6 suggests a higher risk of cardiovascular disease (CVD). The model produces segmented images with distinct boundaries and CDR values, facilitating automated CVD risk assessment from retinal fundus images, which improves both screening efficiency and accuracy.

TABLE II
PERFORMANCE COMPARISON OF DIFFERENT MODELS

Model	Precision	Recall	F1 Score
YOLO			
Optic Cup	0.8012	0.8393	0.8150
Optic Disc	0.8950	0.8948	0.8949
YOLO+FOCALELOU			
Optic Cup	0.9013	0.8693	0.8850
Optic Disc	0.9972	0.9900	0.9936

F. Ophthalmic CVD Indicator

The Ophthalmic CVD Indicator is proposed as a new parameter based on retinal image classification to complement cardiovascular disease (CVD) risk prediction by the inclusion of ophthalmic biomarkers. For the creation of a feature map, STARE dataset is used, which contains retinal fundus images labeled over thirteen different categories, such as Normal(N), Coat Disease(CD), Macroaneurism(MA), Drusen(D), Background Diabetic Retinopathy(BDR), Proliferative Diabetic Retinopathy(PDR), Choroidal Neovascularization(CNV), Arteriosclerotic Retinopathy(AR), Hypertensive Retinopathy(HTR), Central Retinal Vein Occlusion(CRVO), Branch Retinal Vein Occlusion(BRVO), Hemi-Central Retinal Vein Occlusion(HCRVO), and Central/Branch Retinal Artery Occlusion(RAO). These are a range of ophthalmic anomalies that potentially could be key markers of incipient cardiovascular risk factors[14,15,22]. This feature map obtained can be used to augment the final dataset.

G. Fractal Dimension Calculation

Retinal fundus images with the vessels and optic disc already segmented were utilized from our model in order to estimate the Fractal Dimension helping us to indicate the complexity and density of the retinal branching structure. Fractal Dimension provides to be useful in those cases where there is a marginal AV nicking which can sometimes falsely predict CVD. In such situations, using FD as an additional indicator will give a clear sign of CVD risk. For this, we

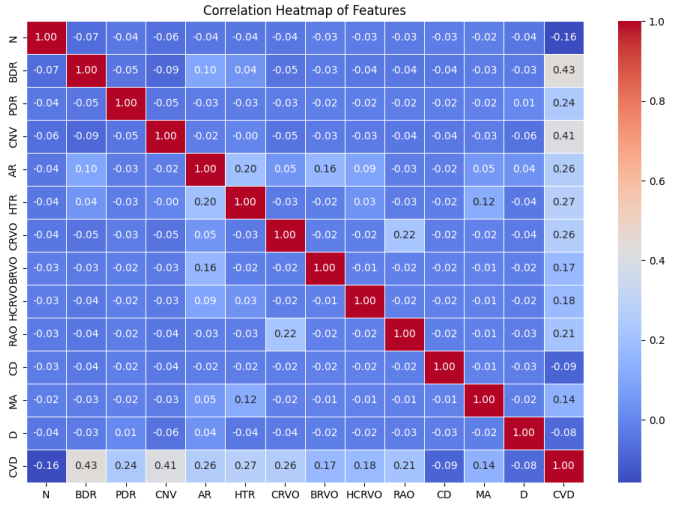

Fig. 4. Correlation of ophthalmic biomarkers to CVD.

follow a particular method where the coordinate system was defined for delimiting three zones from the optic disc: Zone A (0–0.5 disc diameters of the optic disc center), Zone B (0.5–1.0 disc diameters), and Zone C (0.5–2.0 disc diameters).

The box counting method uses box with sizes that are determined using powers of two, ensuring that the image is analyzed at multiple scales to capture its structural complexity. The calculation begins by extracting the height and width of the binary vessel image, which is obtained by segmenting the veins from the retinal image. The minimum of these two dimensions is taken, and its half is used as the upper limit for the largest box size to ensure that the image is not divided into excessively large regions. At each box size, the algorithm reshapes the image into smaller sections of the given size and counts the number of boxes containing at least one vessel pixel. This count is recorded for each box size, and the fractal dimension is estimated by log-log regression of the number of occupied boxes against the inverse of the box size. The resulting slope provides the fractal dimension, which quantifies the vessel network's complexity. A higher fractal dimension (greater than 1.3) suggests a dense, complex branching pattern, indicative of a healthy microvascular network, whereas a lower fractal dimension (less than 1.3) may indicate vessel rarefaction, often associated with conditions like diabetic retinopathy, hypertension, or cardiovascular disease [8].

Using the box counting method, fractal dimension is again the slope of the line when we plot the value of log(N) on the Y-axis against the value of log(r) on the X-axis. The same equation is used to define the fractal dimension, D. This time, N is the number of boxes that cover the pattern, and r is the magnification, or the inverse of the box size.

V. RULE-BASED CVD RISK CLASSIFICATION

Our CVD risk assessment framework employs a **fuzzy rule-based system** that integrates multiple retinal biomarkers to determine cardiovascular risk.

A. Step 1: Define Ophthalmic Biomarkers (OBM)

The presence of high-risk ophthalmic biomarkers is defined as:

$$OBM = BDR \bigvee PDR \bigvee CNV \bigvee ASR \bigvee HR \bigvee CRVO \bigvee BRVO \bigvee HCRVO \bigvee CRAO \bigvee BRAO \bigvee MA$$

B. Step 2: Define AVR Condition

The AVR condition is defined as:

$$AV\_Flag = \begin{cases} 1, & \text{if } AVR < 0.67 \text{ or } AVR > 0.75 \\ 0, & \text{otherwise} \end{cases} \tag{4}$$

C. Step 3: Define CDR Condition

The CDR condition is defined as:

$$CDR\_Flag = \begin{cases} 1, & \text{if } CDR > 0.6 \\ 0, & \text{otherwise} \end{cases} \tag{5}$$

D. Step 4: Define Fractal Dimension Condition

The fractal dimension condition is defined as:

$$FD\_Flag = \begin{cases} 1, & \text{if } FD < 1.3 \\ 0, & \text{otherwise} \end{cases} \tag{6}$$

E. Step 5: Define Neutral Biomarkers (NBM)

Neutral biomarkers, which are not strongly linked to CVD risk, are defined as:

$$NBM = Normal \vee Coat\_Disease \vee Drusen \tag{7}$$

F. Step 6: Compute CVD Risk Based on Conditions

The CVD Risk Classification follows these rules:

- **Rule 1: Direct High-Risk Condition**

$$\text{If } OBM = 1, \quad CVD\_Risk = 1 \tag{8}$$

- **Rule 2: Normal Features + Only Neutral Biomarkers ⇒ Low Risk**

$$\text{If } (NBM = 1) \text{ and } (AVR, CDR, FD \text{ are normal}), \text{ then } CVD\_Risk = 0 \tag{9}$$

- **Rule 3: Neutral Biomarkers + Abnormal Retinal Features ⇒ High Risk**

$$\text{If } (NBM = 1) \text{ and } (AV\_Flag = 1 \vee CDR\_Flag = 1 \vee FD\_Flag = 1), \quad \text{then } CVD\_Risk = 1 \tag{10}$$

- **Rule 4: No Neutral Biomarkers + Any Abnormal Feature ⇒ High Risk**

$$\text{If } (NBM = 1) \text{ and } (AV\_Flag = 1 \vee CDR\_Flag = 1 \vee FD\_Flag = 1), \quad \text{then } CVD\_Risk = 1 \tag{11}$$

G. Final Decision

$$CVD\_Risk = \begin{cases} 1, & \text{if } \begin{array}{l}\text{Any high-risk OBM is present, or} \\ \text{AVR, CDR, or FD abnormalities exist} \\ \text{alongside neutral biomarkers.}\end{array} \\ 0, & \text{if } \begin{array}{l}\text{All features are normal and} \\ \text{only neutral biomarkers are present.}\end{array} \end{cases} \tag{12}$$

VI. Results

To test our system, we utilized several retinal image datasets with varying ophthalmic features, such as predictors of disease risk and diabetic retinopathy. For model evaluation, three datasets were utilized: **RFMiD, Messidor, and EyePACS**, each containing a different number of images. The validation results, including the number of correct classifications and accuracy, are summarized in Table III.

TABLE III
Validation Results on Retinal Image Datasets

Dataset	No. of Images	Correct Classifications	Accuracy (%)
RFMiD	2500	2393	95.72
Messidor	1200	1166	97.21
EyePACS	800	742	92.80

The findings reveal that our system demonstrates **high accuracy across multiple datasets**, confirming its effectiveness in diagnosing retinal images based on disease-related ophthalmic biomarkers. However, the small percentage of misclassified images is likely due to variations in image quality, including outliers, excessive illumination, and poorly captured retinal scans.

As noted in studies such as García et al. [31] and Decenciere et al. [32], public retinal image datasets often contain images with inconsistent illumination, motion artifacts, or blurring, which can affect automated analysis. Despite these challenges, our system maintains strong performance, highlighting its robustness in real-world applications.

VII. Conclusion

This article introduces a model for CVD risk estimation Using retinal fundus images, combining vascular and structural characteristics, natural, and fractal biomarkers. Our approach employs parameters i.e. AV ratio, cup-to-disc ratio,fractal dimension and ophthalamic biomarkers to achieve significantly improved predictive capacity. performance of CVD detection compared to other methods. The The findings confirm the potential value of retinal imaging as a a non-invasive and scalable method for the initial detection of cardiovascular disease. To further ensure the strength and generalizability of Here, we tested our model on various datasets, including like EyePACS, REFUGE, Messidor, and INSPIRE AV for individual features . The excellent accuracy and reproducibility of our results on these Multidatasets validate again the clinic relevance of our recommended strategy.

VIII. Discussion

In this research, we have constructed and evaluated a cardiovascular disease (CVD) risk prediction system using retinal image analysis. Our system combines vessel-based features like Arteriovenous Ratio (AVR), Cup-to-Disc Ratio (CDR), and Fractal Dimension (FD) with ophthalmic biomarkers to measure the occurrence of disease-related abnormalities.

To date, our system includes manually provided ophthalmic The major restriction that goes along with this, though, is that These biomarkers must be extracted first. A critical area One area of future research is the development of an automated feature. extraction method which can identify and quantifying ophthalmic biomarkers from retinal images. This would increase the system's scalability, thus minimizing the importance of manual intervention, and enable real-time CVD risk analysis from raw retinal images.

REFERENCES

[1] Author(s), "A Multi-Stage Approach for Cardiovascular Risk Assessment from Retinal Images," in Proceedings of [Conference Name], Year, pp. XX-XX. DOI: [].

[2] A. Rani and D. Mittal, "Measurement of Arterio-Venous Ratio for Detection of Hypertensive Retinopathy through Digital Color Fundus Images," in Journal of Biomedical Engineering and Medical Imaging, vol. 2, no. 5, pp. 35-45, Oct. 2015. DOI: 10.14738/jbemi.25.1577.

[3] R. Manjunatha and H. S. Sheshadri, "Boundary Extraction and Vessel Width Calculation in Retinal Fundus Images," in Asian Journal of Engineering and Applied Technology, vol. 8, no. 2, pp. 63-70, 2019.

[4] X. R. Gao, F. Wu, P. T. Yuhas, R. K. Rasel, and M. Chiariglione, "Automated Vertical Cup-to-Disc Ratio Determination from Fundus Images for Glaucoma Detection," in Scientific Reports, vol. 14, no. 4494, 2024. DOI: 10.1038/s41598-024-55056-y.

[5] Author(s), "YOLOv8-Based Segmentation of Optic Disc and Cup for Glaucoma Detection," in [Journal/Conference Name], Year, pp. XX-XX. DOI: [].

[6] J. Morano, G. Aresta, and H. Bogunović, "RRWNet: Recursive Refinement Network for Effective Retinal Artery/Vein Segmentation and Classification," in Elsevier Preprint, 2024. DOI: [].

[7] Kiruthika, M & T R, Swapna & Kumar, C. & Peeyush, K.P. (2019). Artery and Vein classification for hypertensive retinopathy. 244-248. 10.1109/ICOEI.2019.8862719..

[8] S. Dinesen et al., "Retinal Vascular Fractal Dimensions and Their Association with Macrovascular Cardiac Disease," in Ophthalmic Research, vol. 64, no. 4, pp. 561–566, 2021. DOI: 10.1159/000514442.

[9] Author(s), "A Multi-Stage Approach for Cardiovascular Risk Assessment from Retinal Images," in Proceedings of [Conference Name], Year, pp. XX-XX. DOI: [if available].

[10] A. Rani and D. Mittal, "Measurement of Arterio-Venous Ratio for Detection of Hypertensive Retinopathy through Digital Color Fundus Images," in Journal of Biomedical Engineering and Medical Imaging, vol. 2, no. 5, pp. 35-45, Oct. 2015. DOI: 10.14738/jbemi.25.1577

[11] R. Manjunatha and H. S. Sheshadri, "Boundary Extraction and Vessel Width Calculation in Retinal Fundus Images," in Asian Journal of Engineering and Applied Technology, vol. 8, no. 2, pp. 63-70, 2019.

[12] X. R. Gao, F. Wu, P. T. Yuhas, R. K. Rasel, and M. Chiariglione, "Automated Vertical Cup-to-Disc Ratio Determination from Fundus Images for Glaucoma Detection," in Scientific Reports, vol. 14, no. 4494, 2024. DOI: 10.1038/s41598-024-55056-y.

[13] Author(s), "YOLOv8-Based Segmentation of Optic Disc and Cup for Glaucoma Detection," in [Journal/Conference Name], Year, pp. XX-XX. DOI:

[14] M. Lyu et al., "Clinical Significance of Subclinical Atherosclerosis in Retinal Vein Occlusion," in Scientific Reports, vol. 11, 2021. DOI: 10.1038/s41598-021-91401-1.

[15] N. Cheung et al., "Diabetic Retinopathy and the Risk of Coronary Heart Disease," in Diabetes Care, vol. 30, no. 7, pp. 1742-1746, 2007. DOI: 10.2337/dc07-0264.

[16] Erwin, R. Zulfahmi, D. S. Noviyanti, G. R. Utami, A. N. Harison and P. S. Agung, "Improved Image Quality Retinal Fundus with Contrast Limited Adaptive Histogram Equalization and Filter Variation," 2019 International Conference on Informatics, Multimedia, Cyber and Information System (ICIMCIS), Jakarta, Indonesia, 2019, pp. 49-54, doi: 10.1109/ICIMCIS48181.2019.8985198. keywords: Enhancement;CLAHE;Median Filter;Wiener Filter;Gaussian Filter,

[17] P. Li, Q. Deng and H. Li, "The Arteriovenous Classification in Retinal Images by U-net and Tracking Algorithm," 2020 IEEE 5th International Conference on Image, Vision and Computing (ICIVC), Beijing, China, 2020, pp. 182-187, doi: 10.1109/ICIVC50857.2020.9177446. keywords: Retina;Image segmentation;Feature extraction;Classification algorithms;Veins;Arteries;Biomedical imaging;artery and vein classification;U-net;vessel tracking,

[18] Ronneberger, O., Fischer, P., Brox, T. (2015). U-Net: Convolutional Networks for Biomedical Image Segmentation. In: Navab, N., Hornegger, J., Wells, W., Frangi, A. (eds) Medical Image Computing and Computer-Assisted Intervention – MICCAI 2015. MICCAI 2015. Lecture Notes in Computer Science(), vol 9351. Springer, Cham. https://doi.org/10.1007/978-3-319-24574-4__28

[19] Zhou Z, Siddiquee MMR, Tajbakhsh N, Liang J. UNet++: A Nested U-Net Architecture for Medical Image Segmentation. *Deep Learning in Medical Image Analysis and Multimodal Learning for Clinical Decision Support*, 2018; **11045**:3-11. doi: 10.1007/978-3-030-00889-5_1.

[20] Hu J, Wang H, Cao Z, Wu G, Jonas JB, Wang YX and Zhang J (2021) Automatic Artery/Vein Classification Using a Vessel-Constraint Network for Multicenter Fundus Images. Front. Cell Dev. Biol. 9:659941. doi: 10.3389/fcell.2021.659941

[21] Chen, N., Lv, X. Research on segmentation model of optic disc and optic cup in fundus. *BMC Ophthalmology*, 2024; **24**:273. doi: 10.1186/s12886-024-03532-4.

[22] Suri MF, Qureshi AI. Hypertensive retinopathy and risk of cardiovascular diseases in a national cohort. *J Vasc Interv Neurol*. 2008 Jul; **1**(3):75-78. PMID: 22518227; PMCID: PMC3317297.

[23] Varghese, R., and S. M. YOLOv8: A Novel Object Detection Algorithm with Enhanced Performance and Robustness. *2024 International Conference on Advances in Data Engineering and Intelligent Computing Systems (ADICS)*, Chennai, India, 2024, pp. 1-6. doi: 10.1109/ADICS58448.2024.10533619.

[24] T. Y. Wong, R. Klein, B. E. Klein, et al., "Retinal microvascular abnormalities and stroke," *Lancet*, vol. 361, no. 9353, pp. 807–808, 2004.

[25] A. R. Sharrett, J. D. Mosley, T. Y. Wong, et al., "Atherosclerosis Risk in Communities Study: Retinal arteriolar narrowing and cardiovascular mortality," *Stroke*, vol. 34, no. 2, pp. 411-416, 2003.

[26] N. Cheung, T. Y. Wong, et al., "Retinal arteriolar narrowing and left ventricular hypertrophy," *Circulation*, vol. 120, no. 5, pp. 543-550, 2009.

[27] H. Hu, et al., "Retinal Vein Occlusion and Stroke Risk: A Meta-Analysis," *Neurology*, vol. 64, no. 4, pp. 801-807, 2005.

[28] I. B. Christoffersen, et al., "Retinal vein occlusion and cardiovascular risk," *British Journal of Ophthalmology*, vol. 95, no. 5, pp. 663-666, 2011.

[29] T. Y. Wong, et al., "Retinal arteriolar narrowing and risk of hypertension and stroke," *Circulation*, vol. 106, no. 8, pp. 963-969, 2002.

[30] M. Ikram, et al., "Retinal Vessel Changes and Hypertension Risk," *Hypertension*, vol. 47, no. 2, pp. 189-195, 2006.

[31] M. O. García, M. G. Penedo, X. M. Pardo, M. G. López, and J. L. Fernández, "Comparison of retinal image quality assessment algorithms in fundus photographs," *Journal of Biomedical Optics*, vol. 22, no. 9, pp. 091507, 2017.

[32] Etienne Decencière, Xiwei Zhang, Guy Cazuguel, Bruno Laÿ, Béatrice Cochener, et al.. FEEDBACK ON A PUBLICLY DISTRIBUTED IMAGE DATABASE: THE MESSIDOR DATABASE. Image Analysis and Stereology, International Society for Stereology, 2014, pp.231-234. 10.5566/ias.1155¿. ¡hal-01082570¿

[33] D. Ghorbanian, S. Jaulim, and A. Chatziralli, "Coats' disease: A review of pathogenesis, clinical presentation, and novel therapeutic approaches," *Journal of Ophthalmology*, vol. 2019, pp. 1-10, 2019.

[34] K. Shields, C. Kaliki, and J. Shields, "Coats disease in adults: Clinical features and treatment outcomes," *Ophthalmology*, vol. 120, no. 7, pp. 1557-1564, 2013.

[35] J. Klein, R. Klein, and B. Meuer, "The epidemiology of age-related macular degeneration: Relationships to cardiovascular disease, risk factors, and lipid metabolism," *Ophthalmology*, vol. 120, no. 3, pp. 457-467, 2013.

[36] C. Curcio, N. Messinger, J. Sloan et al., "Subretinal drusenoid deposits in age-related macular degeneration: Insights from histology and imaging," *Proceedings of the National Academy of Sciences*, vol. 120, no. 4, pp. 1235-1241, 2023.

[37] R. Bressler, A. Munoz, and L. Bressler, "The relationship between drusen and systemic cardiovascular disease: A longitudinal study," *Investigative Ophthalmology Visual Science*, vol. 57, no. 5, pp. 2031-2037, 2016.